
Match What Matters: Generative Implicit Feature Replay for Continual Learning

Kevin Thandiackal^{1,2}, Tiziano Portenier², Andrea Giovannini¹
 Maria Gabrani¹, Orcun Goksel^{2,3}

¹IBM Research Europe, Switzerland

²Computer-assisted Applications in Medicine, ETH Zurich, Switzerland

³Department of Information Technology, Uppsala University, Sweden

Abstract

Neural networks are prone to catastrophic forgetting when trained incrementally on different tasks. In order to prevent forgetting, most existing methods retain a small subset of previously seen samples, which in turn can be used for joint training with new tasks. While this is indeed effective, it may not always be possible to store such samples, e.g., due to data protection regulations. In these cases, one can instead employ generative models to create artificial samples or features representing memories from previous tasks. Following a similar direction, we propose GenIFeR (Generative Implicit Feature Replay) for class-incremental learning. The main idea is to train a generative adversarial network (GAN) to generate images that contain *realistic* features. While the generator creates images at full resolution, the discriminator only sees the corresponding features extracted by the continually trained classifier. Since the classifier compresses raw images into features that are actually relevant for classification, the GAN can match this target distribution more accurately. On the other hand, allowing the generator to create full resolution images has several benefits: In contrast to previous approaches, the feature extractor of the classifier does not have to be frozen. In addition, we can employ augmentations on generated images, which not only boosts classification performance, but also mitigates discriminator overfitting during GAN training. We empirically show that GenIFeR is superior to both conventional generative image and feature replay. In particular, we significantly outperform the state-of-the-art in generative replay for various settings on the CIFAR-100 and CUB-200 datasets.

1 Introduction

Humans have the innate ability to continuously learn new tasks while remembering and leveraging prior knowledge. Similarly, it has been shown that neural networks are able to transfer knowledge from one task to another [1]. Unlike humans, however, when neural networks are fine-tuned on a new task, they suffer from a phenomenon called *catastrophic forgetting* [2, 3]. They immediately forget how to solve previously learned tasks when trained on subsequent ones. This very problem lies at the core of Continual Learning (CL) [4–7]. In particular, CL explores scenarios in which a neural network sequentially learns different tasks, with the restriction that data from previous tasks cannot be kept for future training. These settings simulate real world constraints where data providers cannot grant unlimited and indefinite access to their data. This is especially relevant for confidential or privacy-regulated data, e.g., personal or medical patient data.

In this work, we focus on class-incremental learning (CIL) – a problem setting where a neural network is to incrementally learn different classification tasks [8, 9]. The vast majority of techniques proposed

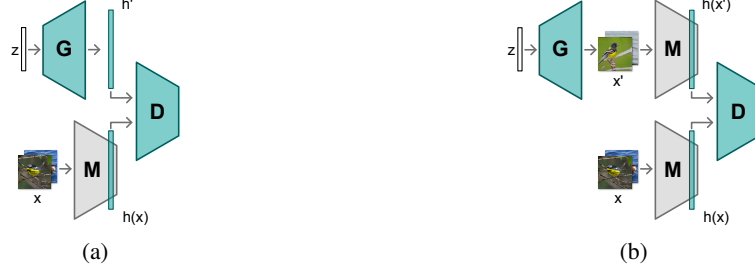


Figure 1: Generative feature matching architectures. The diagrams show how the generator G , the discriminator D , and the model M interact in (a) conventional direct and (b) the proposed indirect feature matching.

to tackle CIL employs some form of training data replay, i.e., a subset of samples from previous tasks to be used for joint training with new tasks [10–15]. While these methods provide effective remedies against catastrophic forgetting, they, strictly speaking, violate the CL constraints and are thus not applicable in scenarios where data from previous tasks is unavailable. This violation can be circumvented by leveraging generative models, e.g., by training variational auto-encoders (VAEs) [16] or generative adversarial networks (GANs) [17] to synthesize artificial samples mimicking the previous tasks. These samples can then be replayed during the training of new tasks.

The above strategy, however, implies training not only a classifier but also a generative model in a continual fashion, which further complicates the learning problem. Therefore, researchers have recently proposed to simplify the generative problem by learning the synthesis of deep features as opposed to raw training images [18–21]. Such generative *feature replay* has emerged as a promising alternative to conventional generative (image) replay, since replacing the manifold of raw training images with the representation learned by a classifier can simplify the target distribution for a generative model. Yet, this approach has a caveat, as the generated features can only mitigate forgetting in deeper classifier representations, implying that the feature extractor itself must not change during training. Therefore, most such techniques leverage frozen pretrained feature extractors [19, 21], which comes at the cost of restricting the classifier’s ability to learn new tasks and hence necessitating sufficient and careful pretraining.

In this work, we propose to overcome these limitations by matching deep features in an indirect manner (see Figure 1). This in turn enables us to employ generative *implicit feature replay* during classifier training. In particular, we train a GAN generator to synthesize training images, while the discriminator only sees the representation learned by the classifier, which forces the generator to create samples that invoke a “realistic” classifier response. This approach combines the advantages of both feature and image replay. First, the complexity of the distribution to be generated is reduced, similarly to conventional feature replay. Second, as in image replay, the classifier also remains fully trainable during CL, enabling effective learning of new tasks. In addition, our approach allows us to leverage image-level augmentations to prevent overfitting in both the classifier and the discriminator, which is not possible with conventional generative feature replay.

2 Related work

Most CL approaches rely on either *regularization*, *isolated parameters*, *experience replay*, or a combination thereof [7]. Many of the early CL methods [22–24] employ some form of prior-focused regularization and penalize changes in the classifier weights that are deemed important for previous tasks. At inference time, these methods rely on knowledge of the task membership of a given sample. However, in real world applications where the task associated to an unseen sample is typically unknown, such approaches suffer from catastrophic forgetting [5, 6]. Another popular CL strategy is parameter isolation, where methods try to prevent forgetting by design, e.g., using fixed networks with learnable masks on their weights [25, 26]. As with regularization-based techniques, these methods typically require task membership information at test time. The recently proposed SupSup model [27] tries to avoid this limitation using a dedicated task inference technique. However, a continually trained classifier never sees data from different tasks simultaneously, rendering it unable to learn class relations across different tasks.

To learn this inter-task relationship, related work proposed to replay previous samples during the training of new tasks, which has proven to be effective [19, 28, 29]. Such a replay mechanism can be implemented with either real (*exemplar replay*) or artificial samples (*generative replay*). iCaRL [10] was among the first proposed exemplar replay methods, using selectively stored exemplars together with a nearest-mean classifier. A major problem with storing a small subset of exemplars is the resulting imbalance between previous and current data, which several methods have tried to address [11, 13, 12, 14]. More recently, approaches inspired by meta-learning have become increasingly popular in CIL [30, 15], resulting in state-of-the-art performance on common benchmarks [31]. Despite these promising results, such exemplar replay based techniques are often not applicable in practice, particularly in scenarios where previous data is inaccessible once learned. Moreover, even in applications where this strong constraint is relaxed, addressing the imbalance between previous exemplars and current samples is non-trivial.

Both aforementioned problems can be circumvented by leveraging generative replay. Once a generative model is trained, the training data is no longer required. Furthermore, such models by definition allow sampling, effectively mitigating any sample imbalance problem. Generative replay using GANs was pioneered in DGR [32], demonstrating feasibility on semi-complex datasets. Wu et al. [33] later pointed out that naïvely leveraging GANs mostly shifts the problem of catastrophic forgetting from the classifier to the generative model, and proposed a generator distillation approach to mitigate forgetting in the generative model. However, pure generator distillation can lead to increasingly corrupted samples over long task sequences [34]. Another strategy against generator forgetting (inspired by parameter isolation) is to expand the generator over time using task-specific parameters. DGM [35] followed this approach and proposed learnable neural masks to prevent changes in generator parameters that are important for previous tasks. Cong et al. [34] also employed model expansion and added task-specific style parameters to a “well-behaved” pretrained GAN, showing that this approach does not suffer from samples being gradually corrupted. In order to scale up to long task sequences, these methods require dedicated compression mechanisms, e.g., enforcing sparse masks [35] or using singular value decomposition for task-specific parameters [34].

Continually learning to generate realistic images is exceedingly difficult. Previous works have therefore proposed to synthesize corresponding classifier features instead, which can greatly reduce the complexity of the distribution to learn. Apart from simplifying the training for generative models, feature replay is further motivated by its parallels to the brain, which also does not pass on mental images back to the retina [19]. Accordingly, in the brain-inspired BI-R [19], a VAE and a classifier were merged into a single model that internally replayed previously learned feature representations. FearNet [18] was another brain-inspired technique that consisted of short- and long-term memory modules combined with a mechanism for generative feature replay. Unlike these brain-inspired approaches, Liu et al. [20] employed a conditional GAN [36] for feature matching. They further introduced a feature distillation loss in the classifier to mitigate forgetting in the feature extractor. However, since this feature distillation loss must be computed on current samples, the classifier representation of previous data is still exposed to changes over time. Moreover, distilling classifier features on current samples conflicts with the goal of learning new classification tasks. Similarly to [20], ILCAN [21] used a conditional GAN to generate synthetic features. However, their generator was not conditioned on class labels, but instead on discriminative feature embeddings that are extracted by the classifier. They found this coupling between the classifier embeddings and the generator input to be beneficial for incremental learning. Note that ILCAN (as well as BI-R and FearNet) relied on a pretrained frozen feature extractor.

In this work, we propose an approach that does neither rely on a frozen feature extractor nor on feature distillation. Thanks to this additional flexibility, our classifier can learn new tasks more easily, while simultaneously retaining previously acquired knowledge. These aspects together result in improved CL performance. In addition, by encoding the classifier features in the image domain, image-based augmentations can be leveraged, which mitigates overfitting in both the classifier and the discriminator. This is particularly effective in limited data scenarios that typically occur in long task sequences with small task sizes.

3 Generative implicit feature replay

In a classical supervised learning problem with i.i.d. data, a classifier is trained on a set sampled from the distribution $\mathcal{S} = \mathcal{X} \times \mathcal{C}$ containing samples $(\mathbf{x}, y) \in \mathcal{S}$ from all classes $y \in \mathcal{C} = \{1, \dots, C\}$. In a

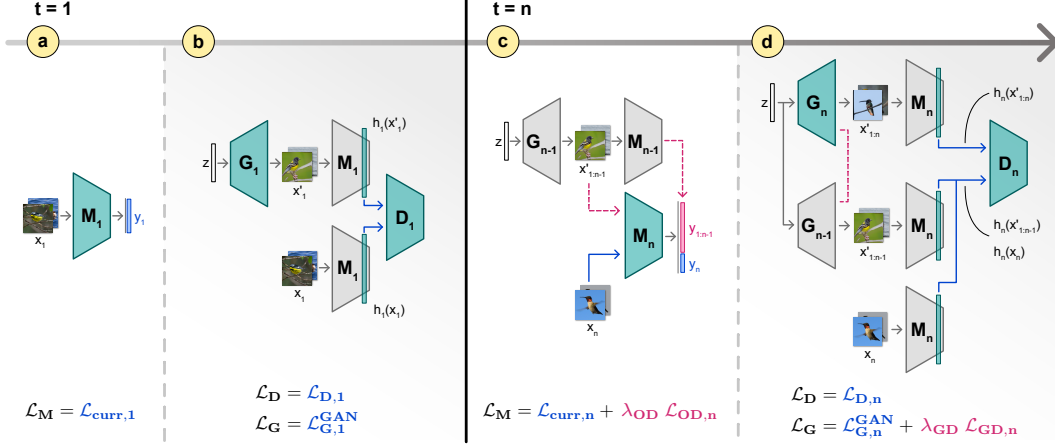


Figure 2: Continual classifier and GAN training, where green represents trainable models and gray indicates frozen models. **(a)** First, the classifier M_1 learns the task 1 on real images x_1 with the classification loss $\mathcal{L}_{curr,1}$. **(b)** Then, the generator G_1 and the discriminator D_1 are trained. G_1 tries to fool D_1 by generating images x'_1 that have realistic features $h_1(x'_1)$. **(c)** For any future task $t = n$, M_n is first initialized from M_{n-1} and then learns to classify current images x_n by optimizing $\mathcal{L}_{curr,n}$ (blue), while previous tasks are remembered by minimizing the output distillation loss $\mathcal{L}_{OD,n}$ (magenta) on synthetic images from G_{n-1} . **(d)** Then, a generator G_n and a discriminator D_n are initialized from G_{n-1} and D_{n-1} , respectively. They are trained with the corresponding GAN losses (blue) such that G_n produces images $x'_{1:n}$ that represent all seen tasks. This includes current real images x_n and previous synthetic images $x'_{1:n-1}$. In addition, a generator distillation loss $\mathcal{L}_{GD,n}$ (magenta) encourages G_n to produce the same previous task images as G_{n-1} .

CIL setting however, we are presented with a partition of \mathcal{S} consisting of subsets $\mathcal{S}_t = \mathcal{X}_t \times \mathcal{C}_t$, where $t \in \mathcal{T} = \{1, \dots, T\}$ indicates a point in time, i.e., $\bigcup_{t \in \mathcal{T}} \mathcal{S}_t = \mathcal{S}$. Since $\{\mathcal{S}_t \mid t \in \mathcal{T}\}$ are disjoint, each subset \mathcal{S}_t contains samples belonging to a unique set of classes \mathcal{C}_t , and we refer to learning \mathcal{S}_t at time t as *task* t .

Our goal is to train a classifier on a sequence of different tasks without access to previous data. To achieve this goal, we propose a novel framework that we call GenIFeR (**Generative Implicit Feature Replay**). It consists of two main components: a classifier and a GAN, trained in an alternating fashion. The purpose of the GAN is to prevent the classifier from forgetting previously learned tasks. The classifier is defined as $M : x \mapsto g(h(x))$, where h is a function that extracts features up to a certain convolutional layer in M , and g maps this representation to output logits for each class. We employ a conditional GAN [37] consisting of a generator G and a discriminator D . Given a class y and a random noise vector z , the generator $G : (z, y) \mapsto x'$ learns to create synthetic images x' from class y . During training, G aims to fool the discriminator D , which in turn learns to distinguish real features $h(x)$ from synthetic features $h(x')$. The sequential process of alternating training is illustrated in Figure 2 for the first task $t = 1$ and an arbitrary future task $t = n$. Note that in our approach, after task $n - 1$, we only retain the classifier M_{n-1} , generator G_{n-1} , and discriminator D_{n-1} in order to proceed to the next task n , i.e., no copies of earlier models need to be stored.

3.1 Classifier training

When learning a new task $t=n$ consisting of L classes, the previous classifier M_{n-1} has been trained on $\mathcal{S}_{1:n-1} = \mathcal{X}_{1:n-1} \times \mathcal{C}_{1:n-1}$, where $|\mathcal{C}_{1:n-1}| = K$. For a given image $x \in \mathcal{X}_n$ belonging to the new task, we define the k -th logit of the current classifier as $M_{n,k}(x)$. Analogously, for a synthetic image x' belonging to a previously learned task, the k -th logit of the previous classifier is denoted by $M_{n-1,k}(x')$. The corresponding predicted class probabilities $q_{n,k}(x)$ and $q_{n-1,k}(x')$ are defined as:

$$q_{n,k}(x) = \frac{e^{M_{n,k}(x)}}{\sum_{j=1}^{K+L} e^{M_{n,j}(x)}}, \quad q_{n-1,k}(x') = \frac{e^{M_{n-1,k}(x')}}{\sum_{j=1}^K e^{M_{n-1,j}(x')}}. \quad (1)$$

To mitigate forgetting when learning new tasks, M_n minimizes a distillation loss. Knowledge distillation was initially proposed by Hinton et al. [38] and has since become popular in CL [39, 10, 11, 15]. For a synthetic previous image \mathbf{x}' , we define our distillation loss as

$$\mathcal{L}_{OD,n} = - \sum_{k=1}^K q_{n-1,k}(\mathbf{x}') \log(q_{n,k}(\mathbf{x}')) , \quad (2)$$

where OD refers to output distillation. For the current task objective, i.e., the loss function on real samples, we minimize cross-entropy, denoted by \mathcal{L}_{curr} . The final training objective is thus defined as

$$\mathcal{L}_{M,n} = \mathcal{L}_{curr,n} + \lambda_{OD} \mathcal{L}_{OD,n} , \quad (3)$$

where λ_{OD} is a distillation weighting coefficient. We empirically found that using an *adaptive* instead of a constant λ_{OD} is beneficial. Our idea is inspired by recent work in the GAN literature [40], where the probability of applying augmentations changes dynamically according to a certain heuristics (see Section 3.3). For this purpose, we define a target ratio ρ^* between \mathcal{L}_{curr} and $\lambda_{OD} \mathcal{L}_{OD}$. Throughout training, λ_{OD} automatically changes over time to maintain the given target ratio. Note that although we replace a hyperparameter (λ_{OD}) by another one (ρ^*), we find ρ^* to be easier to optimize in practice, while yielding superior results (see Section 5.2).

3.2 GAN training

Since we perform indirect feature matching, G synthesizes samples in the image domain, while D must learn to distinguish between features of synthetic images and features of real images. However, as shown in Figure 2(d), the features that are considered as real by D actually comprise both current real and previous synthetic features. More formally, for task n the corresponding set of surrogate images is defined as $\tilde{\mathcal{X}}_n = \mathcal{X}_n \cup \mathcal{X}'_{1:n-1}$. The discriminator loss can then be written as

$$\mathcal{L}_{D,n} = \mathbb{E}_{\substack{\mathbf{z} \sim p_z \\ y \sim p_{C_{1:n}}}} \left[f(D_n(h_n(G_n(\mathbf{z}, y)), y)) \right] + \mathbb{E}_{\mathbf{x}, y \sim p_{\tilde{\mathcal{X}}_n \times C_{1:n}}} \left[f(-D_n(h_n(\mathbf{x}), y)) \right] + R_1(D_n) , \quad (4)$$

where $f(x) = \log(1 + e^x)$ is the softplus function and R_1 [41] represents a gradient penalty that is computed only on the features corresponding to images from the surrogate image set $\mathbf{x} \in \tilde{\mathcal{X}}_n$.

The goal of the generator is to fool D by generating images that result in realistic classifier representations. Accordingly, G minimizes the following loss:

$$\mathcal{L}_{G,n} = \underbrace{\mathbb{E}_{\substack{\mathbf{z} \sim p_z \\ y \sim p_{C_{1:n}}}} \left[f(-D_n(h_n(G_n(\mathbf{z}, y)), y)) \right]}_{\mathcal{L}_{G,n}^{\text{GAN}}} + \lambda_{GD} \underbrace{\mathbb{E}_{\substack{\mathbf{z} \sim p_z \\ y \sim p_{C_{1:n-1}}}} \left[|G_n(\mathbf{z}, y) - G_{n-1}(\mathbf{z}, y)| \right]}_{\mathcal{L}_{GD,n}} . \quad (5)$$

Intuitively, the first term promotes “realism” on the feature level, while the second term encourages G not to forget how to synthesize samples from previously learned classes. The second term can therefore be seen as a form of generator distillation (GD). Note that while the first term is evaluated in the feature space, the second term is computed in the image space.

3.3 Preventing overfitting

When training large networks on small datasets, there is a risk of overfitting to the training samples, which results in poor generalization performance. This pertains not only to classifiers, but also discriminators in GANs. Recently, multiple works [40, 42, 43] identified discriminator overfitting as a root cause for inferior GAN performance on limited training data. As a remedy, Karras et al. proposed an effective pipeline for adaptive discriminator augmentation (ADA). To the best of our knowledge, discriminator overfitting has not been discussed in the context of generative replay for CIL. However, we argue that this aspect is particularly relevant in this scenario, since the dataset sizes per task are typically small in CIL compared to the vast amount of images GANs are usually trained on in non-CIL scenarios.

In our approach, we tackle the problem of discriminator overfitting from two orthogonal directions. First, since we perform indirect feature matching, ADA can be applied on both synthetic and real

images. Note that this is not the case in direct feature matching, since appropriate image-space augmentations are not well defined in feature space. Second, our discriminator loss (Eq. 4) contains not only current real but also previous synthetic features. We found this detail to be crucial, since it effectively prevents the discriminator from becoming too confident, which greatly improves the results. In addition to ADA, indirect feature matching additionally enables us to leverage common image-space augmentations for classifier training such as random cropping and flipping. Note that in the case of direct feature matching, such augmentations can only be applied to current task samples, while our approach can leverage them also in the distillation component. We have found this approach to reduce forgetting by mitigating overfitting to the current task.

4 Experiments

We evaluate our method on two popular CIL benchmark datasets, namely CIFAR-100 [44] and CUB-200 [45]. In order to leverage models pretrained on ImageNet [46], we normalize images from both datasets with the known mean and standard deviation of ImageNet.

CIFAR-100 contains 50 000 training images and 10 000 test images, belonging to 100 different object categories. All images are of size 32×32 . **CUB-200** consists of 5 994 training and 5 794 test images grouped into 200 classes of different birds. This amounts to a small set of at most 30 training images per class. Most images are roughly of size 500×500 . Note that due to a small overlap between ImageNet and CUB-200, we excluded 43 images from the CUB-200 test set.

4.1 Implementation

To evaluate the incremental learning performance, the datasets were split into different tasks, adopting the setting proposed in the previous works [13, 15, 18, 21, 20], where task $t = 1$ consists of learning half of the classes in the dataset, i.e., 50 classes for CIFAR-100 and 100 classes for CUB-200. The second half of a dataset is then split into equally sized tasks containing either 25, 10, 5, or 2 classes. For a fair comparison with previously reported results, we use the exact same task split.

For both datasets, we train a ResNet-18 [47] initialized with weights pretrained on ImageNet. The classifier is trained using the RAdam optimizer [48] with an initial learning rate of $1e-4$ and a weight decay of $5e-4$. On CIFAR-100, we train the classifier for 50 epochs on each task, where the learning rate is divided by a factor of 5 after 15, 30, and 40 epochs respectively. On CUB-200, each task is trained on for 200 epochs, and analogously, the learning rate is divided by a factor of 5 after 60, 120, and 160 epochs respectively.

Since our classifier is pretrained on images of size 224×224 , we upsample the CIFAR-100 images accordingly. During classifier training, both the real and the synthetic images are augmented using random horizontal flips. For CUB-200, due to the small number of samples per class, we use both horizontal flips and random crops as augmentations. CUB-200 images were first resized such that the shorter side has length 128, and then upsampled to obtain a shorter side length of 256. The reason for this procedure is twofold: First, we found that an upper bound classifier trained on random crops of size 224×224 extracted from 256-short-side images yields a competitive upper bound on this dataset. Second, training our generator to synthesize 128×128 images is significantly faster than doubling the resolution, without compromising the CL accuracy.

Our generator follows an architecture inspired by StyleGAN [49], which we render conditional by feeding class information to the generator and by employing a projection discriminator [37]. Both generator and discriminator are trained using a learning rate of $2.5 \cdot 10^{-3}$. The discriminator further uses mini-batch discrimination and is stabilized with R_1 regularization (see Section 3.2). At inference time (i.e., when sampling from the generator to distill the classifier), we use a generator with averaged parameters [50]. For generator distillation, we set the coefficient λ_{GD} to 10. To mitigate discriminator overfitting, ADA is employed [40]. We empirically found that it is beneficial to limit the probability p of augmentations for the discriminator to 0.5. In such limited-data scenarios, $p > 0.5$ would otherwise trigger relatively soon and lead to leaky augmentations, i.e., the generator would start to synthesize e.g. upside-down images. All models were implemented in PyTorch [51] and trained using a single NVIDIA A100 Tensor Core GPU. Training classifier and GAN on the smallest task in CIFAR-100 takes a bit more than 1 hour, while the largest task on CUB-200 requires 4 hours of training. Please refer to the supplemental material for more implementation details and visualizations.

Table 1: Average incremental accuracies α_{all} on CIFAR-100 and CUB-200. Competitor results are reported from the benchmark experiments in [21].

	CIFAR-100				CUB-200		
Classes per task	25	10	5	2	25	10	5
Upper bound	0.828				0.720		
iCaRL [10]	0.609	0.595	0.572	0.528	0.514	0.505	0.496
EEIL [11]	0.567	0.532	0.497	0.503	0.517	0.509	0.499
FearNet [18]	0.663	0.662	0.625	0.569	0.560	0.533	0.527
ILCAN [21]	0.670	0.671	0.631	0.580	0.576	0.576	0.549
GenIFeR (ours)	0.726	0.736	0.712	0.649	0.649	0.648	0.609

4.2 Results

We evaluate GenIFeR using two metrics: the overall test accuracy $\alpha_{all,T}$ at the end of a sequence with T tasks, i.e., the final accuracy over all classes in the dataset, and the average incremental accuracy $\alpha_{all} = \frac{1}{T-1} \sum_{t=2}^T \alpha_{all,t}$. Note that a normalized version of the latter was introduced by Kemker and Kanan [18], but as pointed out in ILCAN [21], normalizing α_{all} with a low upper bound accuracy (from training on the entire dataset) can result in higher values for this metric despite achieving low overall accuracy. We therefore adopt the formulation presented in ILCAN and report our results accordingly, which also guarantees a fair comparison to our baselines.

The average incremental accuracies α_{all} on CIFAR-100 and CUB-200 for different task sizes are shown in Table 1. When comparing the results for different datasets, note that the same task size effectively results in a different number of learned tasks, or sequence length. With respect to the length of a learned task sequence, one may therefore consider e.g. the 5-class scenario in CIFAR-100 to be comparable to the 10-class scenario in CUB-200, since both task sequences comprise in total 10 tasks. In Table 1, each row represents a different method. The second row shows the upper bound, i.e., the accuracy achieved by our classifier when trained offline on the entire dataset. Our upper bound on CIFAR-100 is the same as in ILCAN, while on CUB-200 our upper-bound is slightly below theirs (0.720 vs. 0.755). iCaRL and EEIL are exemplar-based methods, while FearNet and ILCAN are generative replay approaches achieving state-of-the-art results in the aforementioned settings on CIFAR-100 and CUB-200. In summary, GenIFeR significantly outperforms all baseline methods on both datasets across all task sizes.

In addition to α_{all} , on CIFAR-100 we also report the evolution of $\alpha_{all,t}$ over time for 10 classes per task in comparison to ILCAN, the previous state of the art on this dataset (see Figure 3a). Note that a monotonic decrease over time is to be expected, since a classification problem typically becomes more difficult with an increasing number of classes. However, the largest part of the decrease must be attributable to a forgetting of previously learned tasks. As can be seen in Figure 3a, our method outperforms ILCAN after each added task, while maintaining a relatively flat slope over time.

Finally, we would like to emphasize that iCaRL and EEIL employ ResNet-32 as classifier backbone, while FearNet and ILCAN rely on a pretrained ResNet-50. In contrast, GenIFeR uses a pretrained ResNet-18, which consists of significantly fewer classifier parameters. The fact that we significantly outperform previous state of the art in CIL, even exemplar-based approaches, underlines the effectiveness of our generative replay technique in mitigating catastrophic forgetting.

5 Discussion

In the following sections, we discuss the impact of our proposed contributions, in particular indirect feature matching and adaptive output distillation.

5.1 Indirect feature matching

In order to evaluate the effectiveness of indirect feature matching, we conducted multiple ablation experiments. First, given our network architectures in GenIFeR, we replaced indirect feature matching

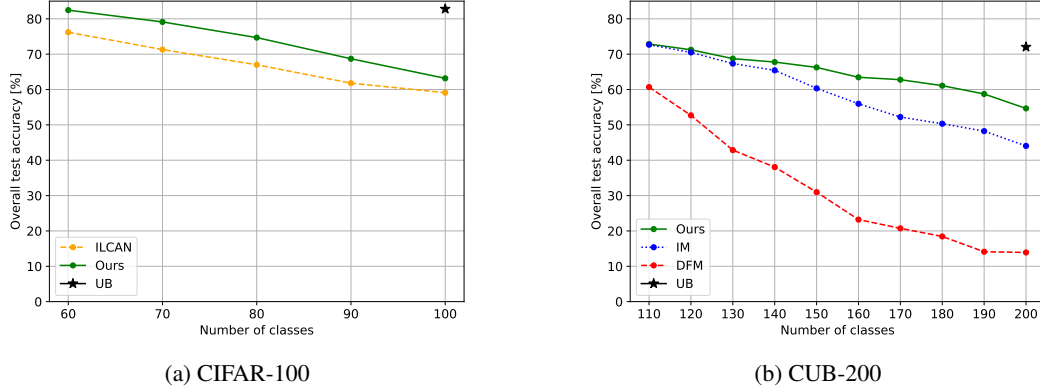


Figure 3: Overall test accuracy (a) for our proposed method GenIFeR vs. ILCAN and the upper bound (UB) on CIFAR-100 with 10 classes per task, and (b) for proposed GenIFeR, image matching (IM), direct feature matching (DFM), and the upper bound (UB) on CUB-200 with 10 classes per task.

Table 2: Average incremental accuracies α_{all} using generative image replay on CUB-200

Classes per task	25	10	5
Constant λ_{OD}	0.577	0.556	0.518
Adaptive λ_{OD}	0.595	0.587	0.548

(IFM) by a direct version (see Figure 1) similarly to [19–21]. This approach is herein called direct feature matching (DFM). To this end, we employed the same discriminator as in IFM, but modified the generator to directly produce features, while maintaining its overall capacity. Note that with DFM, we can neither use ADA for discriminator augmentations, nor augmentations on synthetic data during classifier training. Second, we compare IFM with matching the distribution of raw images (as in [33, 35, 34]), herein called image matching (IM). We used the same generator as for IFM, but adapted the discriminator to distinguish images instead of features, again while maintaining its overall capacity. In contrast to DFM, discriminator augmentations as well as augmentations for the classifier training can still be used in this case.

We empirically found that matching features from the 4th ResNet block works best, which we utilized throughout our experiments on feature matching. Note, however, that other blocks (e.g. block 3) work as well in principle, and we did not perform an exhaustive evaluation thereof. Figure 3b shows the evolution of the overall test accuracy for IFM (ours), IM, and DFM. While IM and IFM are relatively close at the beginning of the task sequence, the discrepancy between them steadily increases as more tasks are learned and IFM clearly outperforms IM at the end. This corroborates the hypothesis that matching a distribution of features is more effective than matching the distribution of raw images, since the distribution becomes increasingly more complex over time. Therefore, IFM becomes increasingly beneficial for longer task sequences, which is an important property in practice. DFM on the other hand clearly performs worst, suffering from catastrophic forgetting already early in the sequence. The most obvious reason for this is that ADA, a technique against discriminator overfitting, cannot be applied in feature space, since it is defined in image space. Since a CUB-200 task in this setting corresponds to only 300 images in the training set, D overfitting is unavoidable. Another reason for the strong contrast to both IM and IFM is the fact that the feature extractor in DFM must be frozen up to the matching ResNet block in order to avoid catastrophic forgetting in the network parameters before the matching layer. This leaves little capacity in the remaining layers to learn new tasks without forgetting previously learned tasks.

5.2 Adaptive output distillation

Finally, we show results of our proposed adaptive output distillation coefficient in comparison to grid-searched constant coefficients on various task sizes. To this end, we evaluate the average incremental

accuracy for generative image replay on CUB-200. We use image replay as opposed to feature replay for these experiments, since in image replay, the generator is decoupled from the classifier, which enables us to perform a grid search of λ_{OD} without re-training the GAN on the entire task sequence for each value of λ_{OD} . However, we found that the conclusions also apply on feature replay, although we did not perform an extensive evaluation in the form of a fine-grained grid search.

As shown in Table 2, using an adaptive λ_{OD} leads to better results across all task sizes, compared to grid-searched constant coefficients. While we were able to achieve these results using a single ρ^* , the optimal grid-searched constant λ_{OD} is different for different task sizes. We conjecture that the main advantage of an adaptive coefficient comes from the fact that the coefficient can be low in situations where the previous tasks are already remembered well, whereas it can increase when there is a need to put more emphasis on remembering old task compared to learning new tasks. This flexibility seems to be advantageous in CIL, since over long task sequences, different tasks exhibit varying levels of difficulty and new and old classes have varying amount of features in common. Thus, remembering previous tasks while learning new ones may involve a varying level of difficulty in different scenarios and at different stages. A potential disadvantage of the adaptive coefficient for any defined value ρ^* is that in some cases, e.g., when for some reason a new task cannot be learned at all, the coefficient may keep rising in order to achieve the targeted loss ratio ρ^* . In practice, such a scenario is effectively avoided by clamping λ_{OD} to a maximum value of 100. As long as the coefficient is not constantly at this maximum, we can always benefit from a distillation loss that is only weighted as much as is necessary.

6 Conclusions

We have proposed generative implicit feature replay for CIL. This novel framework has several advantages compared to previously proposed methods. In contrast to exemplar-based approaches, we do not require storing any real samples. Therefore, our method can be applied in real-world scenarios, including those with confidentiality or patient-privacy concerns. We have also showed that the concept of indirect feature matching is superior to direct feature matching as well as image matching. By matching feature representations while generating raw images, we are able to combine the best of these two worlds: First, matching the distribution of features is easier for a GAN, which becomes increasingly important for longer task sequences. Second, by generating images, we can benefit from image-level augmentations, which helps to reduce overfitting in both the classifier as well as the discriminator.

7 On potential negative societal impacts

Developing a system that is able to continually learn new tasks can have advantages and disadvantages for society. Considering the example of a machine learning (ML) system deployed in the healthcare domain, it is important to be able to regularly update the system and learn from new data. If the system is locked after initial training, there is no way to remove potential biases or errors in the initial training data. On the other hand, if a deployed ML system naively trains on new incoming data without any precautions, additional unwanted biases or even wrong diagnoses may be learned [52]. It is therefore crucial for all stakeholders involved to put in place the necessary safeguards and regulations such that these ML systems can be deployed without exhibiting unexpected and unwanted behavior.

References

- [1] Sinno Jialin Pan and Qiang Yang. A survey on transfer learning. *IEEE Transactions on Knowledge and Data Engineering*, 22(10):1345–1359, 2010. ISSN 10414347. doi: 10.1109/TKDE.2009.191.
- [2] Michael McCloskey and Neal J. Cohen. Catastrophic Interference in Connectionist Networks: The Sequential Learning Problem. In *Psychology of Learning and Motivation*, volume 24, pages 109–165. Academic Press, 1989. ISBN 0079-7421. doi: 10.1016/S0079-7421(08)60536-8.

- [3] Ian J. Goodfellow, Mehdi Mirza, Da Xiao, Aaron Courville, and Yoshua Bengio. An Empirical Investigation of Catastrophic Forgetting in Gradient-Based Neural Networks. *arXiv preprint arXiv:1312.6211*, 2013.
- [4] German I. Parisi, Ronald Kemker, Jose L. Part, Christopher Kanan, and Stefan Wermter. Continual Lifelong Learning with Neural Networks: A Review. *Neural Networks*, 113:54–71, 2019. doi: 10.1016/j.neunet.2019.01.012.
- [5] Sebastian Farquhar and Yarin Gal. Towards Robust Evaluations of Continual Learning. *arXiv preprint arXiv:1805.09733*, 2018.
- [6] Gido M. van de Ven and Andreas S. Tolias. Three scenarios for continual learning. *arXiv preprint arXiv:1904.07734*, 2019.
- [7] Matthias De Lange, Rahaf Aljundi, Marc Masana, Sarah Parisot, Xu Jia, Ales Leonardis, Gregory Slabaugh, and Tinne Tuytelaars. A continual learning survey: Defying forgetting in classification tasks. *IEEE Transactions on Pattern Analysis and Machine Intelligence*, 2021.
- [8] Marc Masana, Xialei Liu, Bartłomiej Twardowski, Mikel Menta, Andrew D. Bagdanov, and Joost van de Weijer. Class-incremental learning: survey and performance evaluation. *arXiv preprint arXiv:2010.15277*, 2020.
- [9] Eden Belouadah, Adrian Popescu, and Ioannis Kanellos. A Comprehensive Study of Class Incremental Learning Algorithms for Visual Tasks. *Neural Networks*, 135:38–54, 2021. ISSN 0893-6080. doi: <https://doi.org/10.1016/j.neunet.2020.12.003>.
- [10] Sylvestre-Alvise Rebuffi, Alexander Kolesnikov, Georg Sperl, and Christoph H. Lampert. iCaRL: Incremental Classifier and Representation Learning. In *Proceedings of the IEEE Conference on Computer Vision and Pattern Recognition (CVPR)*, 2017.
- [11] Francisco M Castro, Manuel J Marín-Jiménez, Nicolás Guil, Cordelia Schmid, and Karteek Alahari. End-to-End Incremental Learning. In *Proceedings of the European Conference on Computer Vision (ECCV)*, 2018.
- [12] Yue Wu, Yinpeng Chen, Lijuan Wang, Yuancheng Ye, Zicheng Liu, Yandong Guo, and Yun Fu. Large Scale Incremental Learning. In *Proceedings of the IEEE/CVF Conference on Computer Vision and Pattern Recognition (CVPR)*, 2019.
- [13] Saihui Hou, Xinyu Pan, Chen Change Loy, Zilei Wang, and Dahua Lin. Learning a Unified Classifier Incrementally via Rebalancing. In *Proceedings of the IEEE/CVF Conference on Computer Vision and Pattern Recognition (CVPR)*, 2019.
- [14] Eden Belouadah and Adrian Popescu. ScaIL: Classifier Weights Scaling for Class Incremental Learning. In *Proceedings of the IEEE/CVF Winter Conference on Applications of Computer Vision (WACV)*, 2020.
- [15] Yaoyao Liu, Yuting Su, An-An Liu, Bernt Schiele, and Qianru Sun. Mnemonics Training: Multi-Class Incremental Learning without Forgetting. In *Proceedings of the IEEE/CVF Conference on Computer Vision and Pattern Recognition (CVPR)*, 2020. URL <https://github.com/yaoyao-liu/mnemonics>.
- [16] Diederik P Kingma and Max Welling. Auto-Encoding Variational Bayes. *arXiv preprint arXiv:1312.6114*, 2013.
- [17] Ian J. Goodfellow, Jean Pouget-Abadie, Mehdi Mirza, Bing Xu, David Warde-Farley, Sherjil Ozair, Aaron Courville, and Yoshua Bengio. Generative Adversarial Nets. In *Advances in Neural Information Processing Systems*, volume 27, 2014.
- [18] Ronald Kemker and Christopher Kanan. FearNet: Brain-Inspired Model for Incremental Learning. In *6th International Conference on Learning Representations, ICLR 2018, Vancouver, BC, Canada, April 30 - May 3, 2018, Conference Track Proceedings*, 2018.
- [19] Gido M. van de Ven, Hava T. Siegelmann, and Andreas S. Tolias. Brain-inspired replay for continual learning with artificial neural networks. *Nature Communications*, 11(1), 2020. ISSN 20411723. doi: 10.1038/s41467-020-17866-2.

- [20] Xialei Liu, Chenshen Wu, Mikel Menta, Luis Herranz, Bogdan Raducanu, Andrew D. Bagdanov, Shangling Jui, and Joost van de Weijer. Generative Feature Replay For Class-Incremental Learning. In *Proceedings of the IEEE/CVF Conference on Computer Vision and Pattern Recognition (CVPR) Workshops*, 2020.
- [21] Ye Xiang, Ying Fu, Pan Ji, and Hua Huang. Incremental Learning Using Conditional Adversarial Networks. In *Proceedings of the IEEE/CVF International Conference on Computer Vision (ICCV)*, 2019.
- [22] James Kirkpatrick, Razvan Pascanu, Neil Rabinowitz, Joel Veness, Guillaume Desjardins, Andrei A. Rusu, Milan Kieran, John Quan, Tiago Ramalho, Agnieszka Grabska-Barwinska, Demis Hassabis, Claudia Clopath, Dharshan Kumaran, and Raia Hadsell. Overcoming catastrophic forgetting in neural networks. *Proceedings of the National Academy of Sciences*, 114(13):3521–3526, 2017. doi: 10.1073/pnas.1611835114.
- [23] Cuong V. Nguyen, Yingzhen Li, Thang D. Bui, and Richard E. Turner. Variational Continual Learning. In *6th International Conference on Learning Representations, ICLR 2018, Vancouver, BC, Canada, April 30 - May 3, 2018, Conference Track Proceedings*, 2018.
- [24] Friedemann Zenke, Ben Poole, and Surya Ganguli. Continual Learning Through Synaptic Intelligence. In *Proceedings of the 34th International Conference on Machine Learning*, volume 70 of *Proceedings of Machine Learning Research*, pages 3987–3995, 2017.
- [25] Arun Mallya, Dillon Davis, and Svetlana Lazebnik. Piggyback: Adapting a Single Network to Multiple Tasks by Learning to Mask Weights. In *Proceedings of the European Conference on Computer Vision (ECCV)*, 2018.
- [26] Joan Serra, Dídac Surís, Marius Miron, and Alexandros Karatzoglou. Overcoming catastrophic forgetting with hard attention to the task. In *Proceedings of the 35th International Conference on Machine Learning*, volume 80 of *Proceedings of Machine Learning Research*, pages 4548–4557, 2018.
- [27] Mitchell Wortsman, Vivek Ramanujan, Rosanne Liu, Aniruddha Kembhavi, Mohammad Rastegari, Jason Yosinski, and Ali Farhadi. Supermasks in Superposition. In *Advances in Neural Information Processing Systems*, volume 33, 2020.
- [28] Timothée Lesort. Continual Learning: Tackling Catastrophic Forgetting in Deep Neural Networks with Replay Processes. *arXiv preprint arXiv:2007.00487*, 2020.
- [29] Timothée Lesort, Andrei Stoian, and David Filliat. Regularization Shortcomings for Continual Learning. *arXiv preprint arXiv:1912.03049*, 2019.
- [30] Matthew Riemer, Ignacio Cases, Robert Ajemian, Miao Liu, Irina Rish, Yuhai Tu, and Gerald Tesauro. Learning to Learn without Forgetting By Maximizing Transfer and Minimizing Interference. In *7th International Conference on Learning Representations, ICLR 2019, New Orleans, LA, USA, May 6-9, 2019*, 2019.
- [31] Jathushan Rajasegaran, Salman Khan, Munawar Hayat, Fahad Shahbaz Khan, and Mubarak Shah. iTAML: An Incremental Task-Agnostic Meta-learning Approach. In *Proceedings of the IEEE/CVF Conference on Computer Vision and Pattern Recognition (CVPR)*, 2020.
- [32] Hanul Shin, Jung Kwon Lee, Jaehong Kim, and Jiwon Kim Sk T-Brain. Continual Learning with Deep Generative Replay. In *Advances in Neural Information Processing Systems*, volume 30, 2017.
- [33] Chenshen Wu, Luis Herranz, Xialei Liu, Yaxing Wang, Joost Van De Weijer, and Bogdan Raducanu. Memory Replay GANs: learning to generate images from new categories without forgetting. In *Advances in Neural Information Processing Systems*, volume 31, 2018. URL <https://github.com/WuChenshen/MeRGAN>.
- [34] Yulai Cong, Miaoyun Zhao, Jianqiao Li, Sijia Wang, and Lawrence Carin. GAN Memory with No Forgetting. In *Advances in Neural Information Processing Systems*, volume 33, 2020.

- [35] Oleksiy Ostapenko, Mihai Puscas, Tassilo Klein, Patrick Jähnichen, and Moin Nabi. Learning to Remember: A Synaptic Plasticity Driven Framework for Continual Learning. In *Proceedings of the IEEE/CVF Conference on Computer Vision and Pattern Recognition (CVPR)*, 2019.
- [36] Mehdi Mirza and Simon Osindero. Conditional Generative Adversarial Nets. *arXiv preprint arXiv:1411.1784*, 2014.
- [37] Takeru Miyato and Masanori Koyama. cGANs with Projection Discriminator. *arXiv preprint arXiv:1802.05637*, 2018.
- [38] Geoffrey Hinton, Oriol Vinyals, and Jeff Dean. Distilling the Knowledge in a Neural Network. *arXiv preprint arXiv:1503.02531*, 2015.
- [39] Zhizhong Li and Derek Hoiem. Learning without Forgetting. *IEEE Transactions on Pattern Analysis and Machine Intelligence*, 40(12):2935–2947, 2018. doi: 10.1109/TPAMI.2017.2773081.
- [40] Tero Karras, Miika Aittala, Janne Hellsten, Samuli Laine, Jaakko Lehtinen, and Timo Aila. Training Generative Adversarial Networks with Limited Data. In *Advances in Neural Information Processing Systems*, volume 33, 2020. URL <https://github.com/NVlabs/stylegan2-ada>.
- [41] Lars Mescheder, Andreas Geiger, and Sebastian Nowozin. Which Training Methods for GANs do actually Converge? In *Proceedings of the 35th International Conference on Machine Learning*, volume 80, 2018.
- [42] Zhengli Zhao, Zizhao Zhang, Ting Chen, Sameer Singh, and Han Zhang. Image Augmentations for GAN Training. *arXiv preprint arXiv:2006.02595*, 2020.
- [43] Ngoc-Trung Tran, Viet-Hung Tran, Ngoc-Bao Nguyen, Trung-Kien Nguyen, and Ngai-Man Cheung. On Data Augmentation for GAN Training. *IEEE Transactions on Image Processing*, 30, 2021. doi: 10.1109/TIP.2021.3049346.
- [44] Alex Krizhevsky. Learning Multiple Layers of Features from Tiny Images. Technical report, 2009.
- [45] Catherine Wah, Steve Branson, Peter Welinder, Pietro Perona, and Serge Belongie. The Caltech-UCSD Birds-200-2011 Dataset. Technical report, California Institute of Technology, 2011.
- [46] Olga Russakovsky, Jia Deng, Hao Su, Jonathan Krause, Sanjeev Satheesh, Sean Ma, Zhiheng Huang, Andrej Karpathy, Aditya Khosla, Michael Bernstein, Alexander C. Berg, and Li Fei-Fei. ImageNet Large Scale Visual Recognition Challenge. *International Journal of Computer Vision*, 115(3):211–252, 2015. ISSN 15731405. doi: 10.1007/s11263-015-0816-y.
- [47] Kaiming He, Xiangyu Zhang, Shaoqing Ren, and Jian Sun. Deep Residual Learning for Image Recognition. *2016 IEEE Conference on Computer Vision and Pattern Recognition (CVPR)*, pages 770–778, 2016. ISSN 1664-1078. doi: 10.1109/CVPR.2016.90. URL <http://ieeexplore.ieee.org/document/7780459/>.
- [48] Liyuan Liu, Georgia Tech, Pengcheng He, Weizhu Chen, Xiaodong Liu, Jianfeng Gao, and Jiawei Han. On the Variance of the Adaptive Learning Rate and Beyond. In *8th International Conference on Learning Representations, ICLR 2020, Addis Ababa, Ethiopia, April 26-30, 2020*, 2020. URL <https://github.com/LiyuanLucasLiu/RAdam>.
- [49] Tero Karras, Samuli Laine, Miika Aittala, Janne Hellsten, Jaakko Lehtinen, and Timo Aila. Analyzing and Improving the Image Quality of StyleGAN. In *Proceedings of the IEEE/CVF Conference on Computer Vision and Pattern Recognition*, 2020. URL <https://github.com/NVlabs/stylegan2>.
- [50] Yasin Yazıcı, Chuan-Sheng Foo, Stefan Winkler, Kim-Hui Yap, Georgios Piliouras, and Vijay Chandrasekhar. The Unusual Effectiveness of Averaging in GAN Training. In *7th International Conference on Learning Representations, ICLR 2019, New Orleans, LA, USA, May 6-9, 2019*, 2019.

- [51] Adam Paszke, Sam Gross, Francisco Massa, Adam Lerer, James Bradbury, Gregory Chanan, Trevor Killeen, Zeming Lin, Natalia Gimelshein, Luca Antiga, Alban Desmaison, Andreas Köpf, Edward Yang, Zach DeVito, Martin Raison, Alykhan Tejani, Sasank Chilamkurthy, Benoit Steiner, Lu Fang, Junjie Bai, and Soumith Chintala. PyTorch: An Imperative Style, High-Performance Deep Learning Library. In *Advances in Neural Information Processing Systems*, volume 32, 2019.
- [52] Kerstin N Vokinger, Stefan Feuerriegel, and Aaron S Kesselheim. Continual learning in medical devices: FDA’s action plan and beyond. *The Lancet Digital Health*, 3(6):e337–e338, 6 2021. ISSN 25897500. doi: 10.1016/s2589-7500(21)00076-5.

Supplemental Material

In this supplemental material we present additional results, visualizations, and analyses of GenIFeR, our framework for class-incremental learning. In Appendix A, we first report additional ablation experiments that demonstrate the effectiveness of augmentations. Next, in Appendix B we show sample images of our generative replay. Furthermore, we provide details on the employed generator and discriminator architectures in Appendix C. In Appendix D, the update rule for the adaptive output distillation is explained in detail. Finally, hyperparameter settings for both the classifier and GAN training can be found in Appendix E.1 and Appendix E.2, respectively.

A The effectiveness of augmentations

We conduct an ablation study to evaluate the effectiveness of augmentations for both the classifier as well as the discriminator. To this end, we compare our proposed GenIFeR to configurations, where either no augmentations on previous synthetic images are employed during classifier training, or no ADA (adaptive discriminator augmentation) [40] is employed during GAN training. Figure 4 shows the corresponding evolution of the overall test accuracy for 10 classes per task on CUB-200. We can see that the accuracy drops significantly when either of the augmentations is omitted. Note that both augmentations are essential for the achieved accuracy especially as more tasks are added. This confirms the effectiveness of augmentations for class-incremental learning, in particular for small sized datasets such as CUB-200.

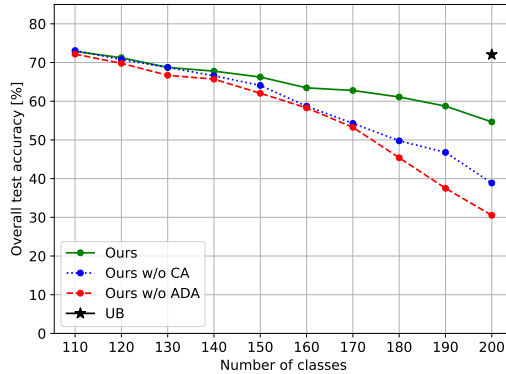


Figure 4: Overall test accuracy for our proposed GenIFeR, without augmentations of previous synthetic images during classifier training (w/o CA), and without augmentations for the discriminator (w/o ADA) on CUB-200 with 10 classes per task.

B Qualitative results

Figure 5 and Figure 6 show example images created by the generator right after pretraining on task $t = 1$.

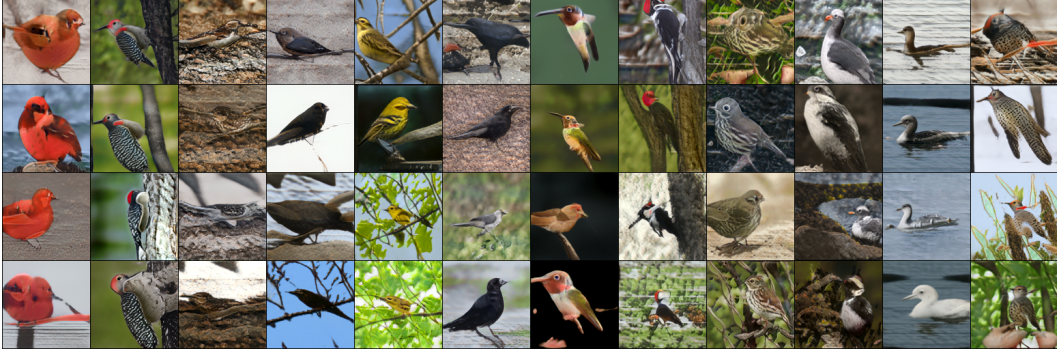


Figure 5: Generated images after pretraining on task ($t = 1$) in CUB-200. Each column shows different samples of one class.

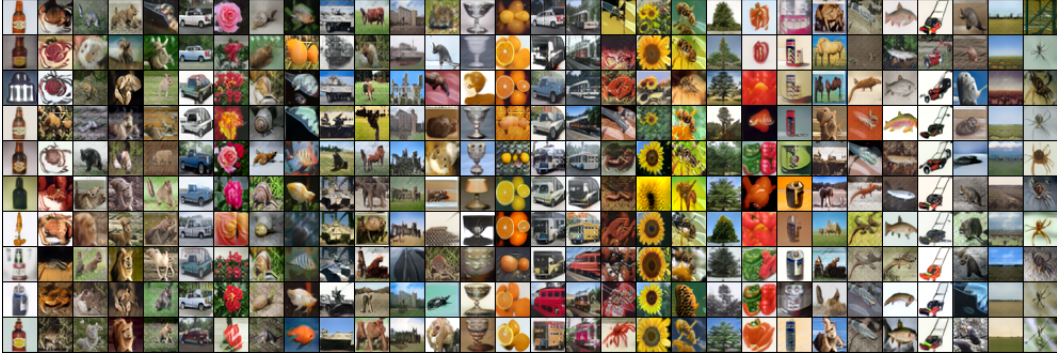


Figure 6: Generated images after pretraining on task ($t = 1$) in CIFAR-100. Each column shows different samples of one class.

Figure 7 and Figure 8 illustrate the continual GAN training for CUB-200 and CIFAR-100, respectively. After learning each task, we show generated images belonging to all tasks seen so far. One can observe that the initially learned task images are not forgotten after a sequence of several tasks, while at the same time, the GAN learns to generate images of new tasks successfully. The former property is further illustrated in Figure 9. It shows that at the end of the task sequence, the generated images for the first task are almost indistinguishable from images generated right after learning this task.

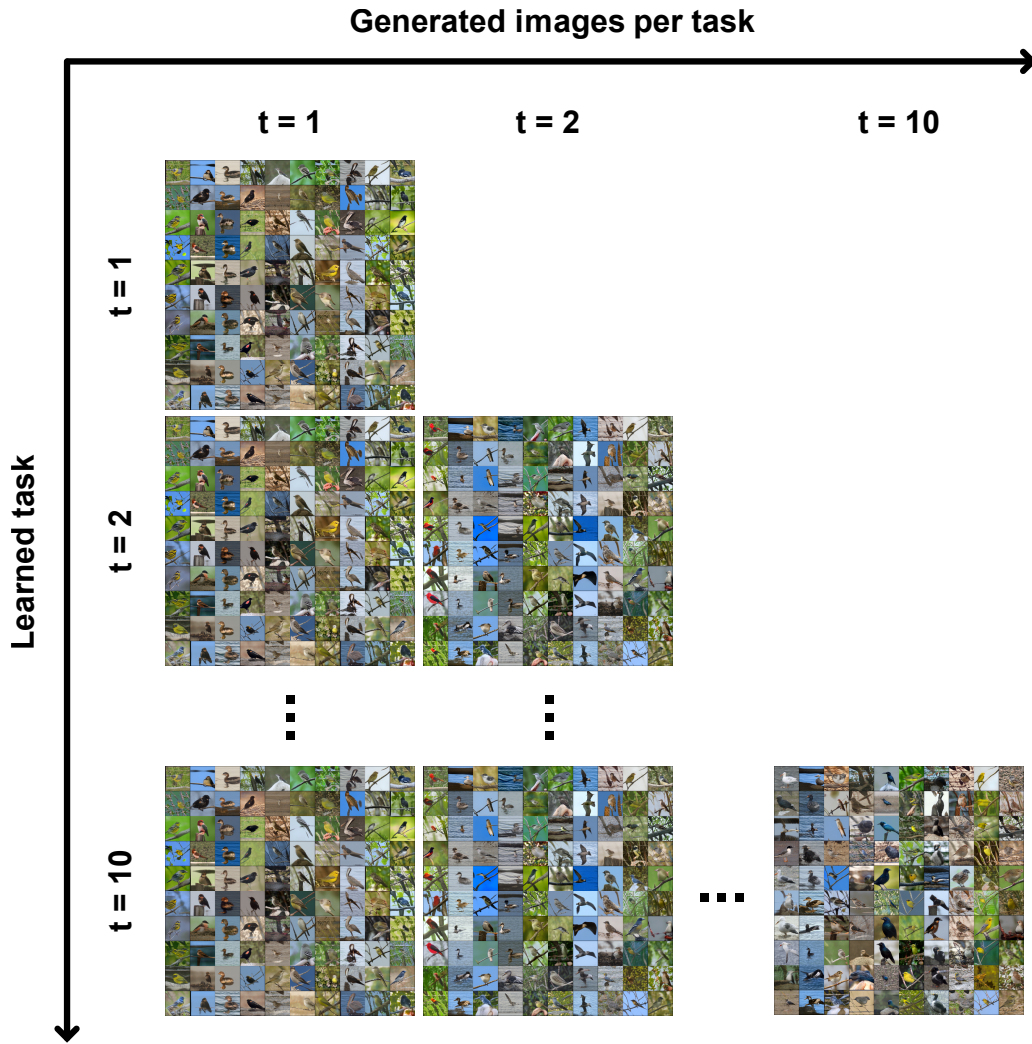


Figure 7: Generated images on CUB-200 for 10 classes per task. In each square of images, one column shows samples of one class. Training progress goes from top to bottom, i.e., the bottom row of squares shows images of task $t \in \{1, 2, \dots, 10\}$ after the GAN has been trained on task $t = 10$. To compare images of the same task at different points in the task sequence, the same random noise inputs are used.

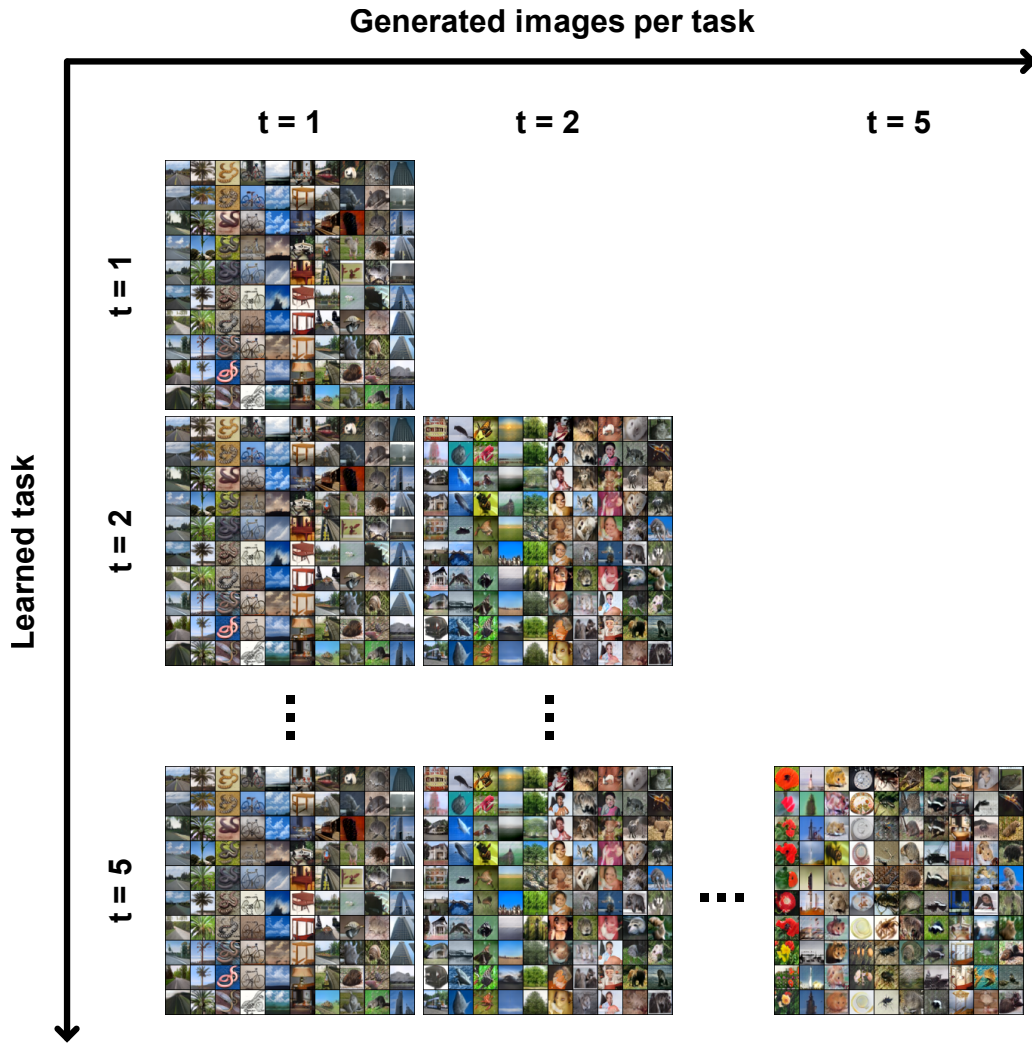


Figure 8: Generated images on CIFAR-100 for 10 classes per task. In each square of images, one column shows samples of one class. Training progress goes from top to bottom, i.e., the bottom row of squares shows images of task $t \in \{1, 2, \dots, 5\}$ after the GAN has been trained on task $t = 5$. To compare images of the same task at different points in the task sequence, the same random noise inputs are used.



(a)



(b)

Figure 9: Detailed view of (a) generated CUB-200 images for $t = 1$ right after training on $t = 1$ and (b) generated images for $t = 1$ after training on $t = 10$. After 10 tasks, only very subtle changes can be observed, e.g., in the eyes of the birds.

C GAN architecture

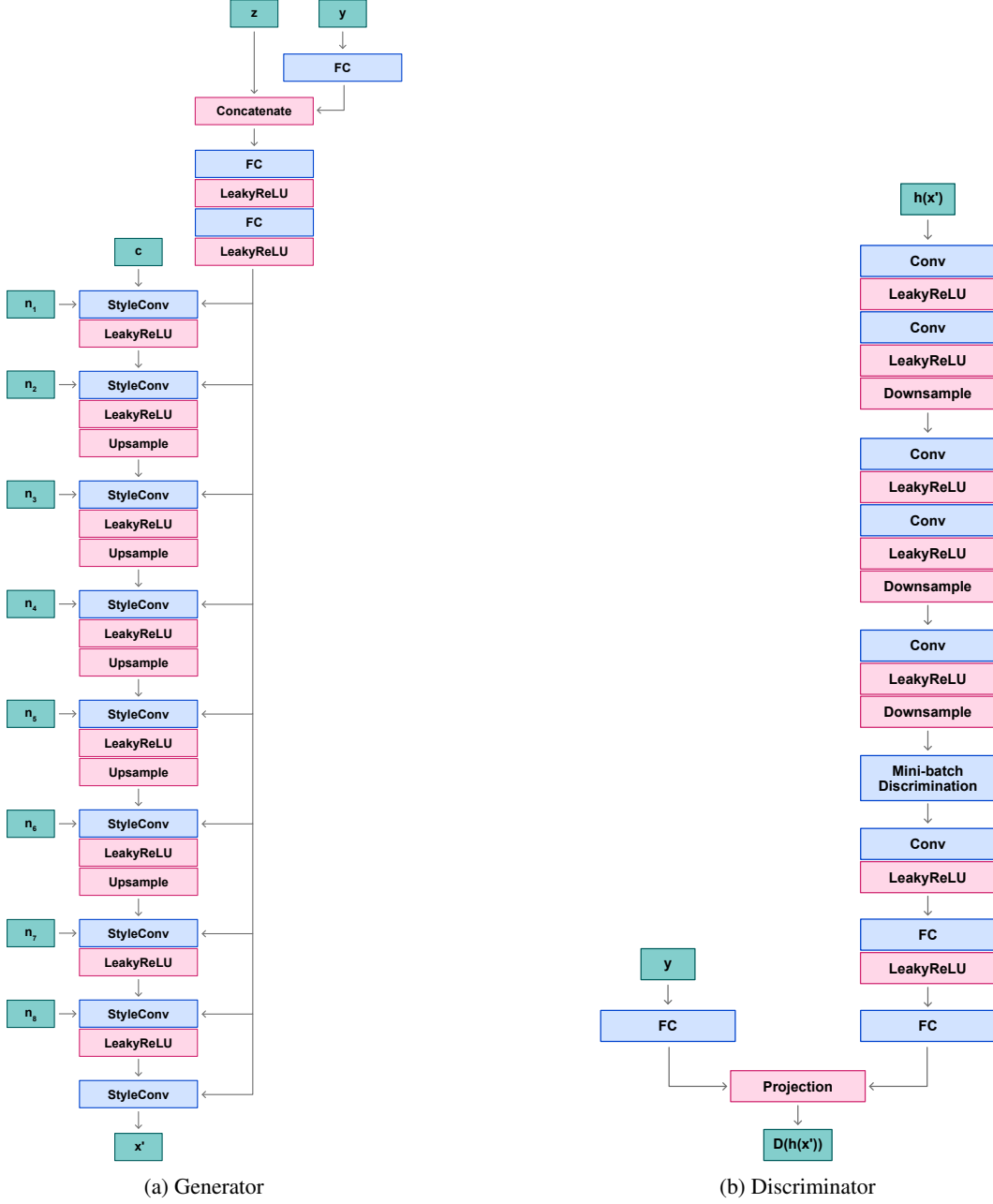


Figure 10: Generator and discriminator architectures. (a) c is a learned input constant, z is the random noise vector input, and n_i are noise maps that are fed to different layers. y is a one-hot vector containing the class information. A StyleConv module consists of style modulation, convolution, and noise injection. FC represents fully-connected layers. (b) The input to the discriminator is $h(x')$, i.e., the feature representation of an image x' .

D Adaptive output distillation

We employ an update rule for the adaptive λ_{OD} similar to the one proposed by Karras et al. [40] for the probability of their adaptive discriminator augmentations. Let i be the index of a batch of images used during classifier training. The output distillation coefficient λ_{OD} is only updated every I batches, i.e., it remains constant between $i + 1$ and $i + I$. Given a target ratio ρ^* between \mathcal{L}_{curr} and $\lambda_{OD} \mathcal{L}_{OD}$, the goal is to modify λ_{OD} such that the estimated current ratio ρ_i (moving average) is close to ρ^* :

$$\lambda_{OD,i+I} = \lambda_{OD,i} + \text{sgn}(\rho_i - \rho^*) \frac{I}{S}$$

$$\rho_i = \frac{1}{I} \sum_{j=i-I+1}^i \frac{\mathcal{L}_{curr}^j}{\lambda_{OD,j} \mathcal{L}_{OD}^j}, \quad (6)$$

where S is a scaling factor for the updates to λ_{OD} . To avoid negative or exceedingly high values, we limit λ_{OD} to a range of $[0, 100]$.

E Hyperparameters

E.1 Classifier

Table 3: Hyperparameters for the classifier training. The batch ratio η denotes the ratio between previous and current samples in a batch.

	CIFAR-100	CUB-200
Epochs per task	50	200
Target loss ratio ρ^*	0.45	0.9
Update interval I	4	
Scaling factor S	10	
Batch size	32	
Batch ratio η	0.5	
Optimizer	RAadam	
Learning rate	0.0001	
Weight decay	0.0005	
$\lambda_{OD,max}$	100	

E.2 GAN

For generator distillation, we use $\lambda_{GD} = 10$ with an additional ratio $\kappa = \frac{n_{prev}}{n_{curr}}$ between the number of previous and current classes. λ_{GD} is then scaled by this factor, in order to increase the emphasis of the generator distillation (in relation to the GAN loss) as more tasks are added. We use $\gamma = 0.1$ for the discriminator’s R_1 regularization (see [41]). As in previous work, we minimize R_1 regularization only every $I_{R_1} = 16$ discriminator steps (referred to as lazy R_1 regularization in [49]). For all settings, we employed a batch size of 64 and a learning rate of 0.0025 for both discriminator and generator. Note that the discriminator is updated once per generator update. Details on the duration of the GAN training for each task size are provided in Table 4.

Table 4: Number of images (multiples of 1000) that the GAN sees during training of one task.

	CIFAR-100					CUB-200			
Classes per task	50 (pretraining)	25	10	5	2	50 (pretraining)	25	10	5
Images seen by GAN per task ($\times 1000$)	16 000	6 400	2 560	1 280	960	16 000	1 920	1 920	1 280